GENERATION OF TUNABLE SUB-FEMTOSECOND XFEL PULSES BY ELECTRON BUNCH RECOMPRESSION USING REVERSE-ENERGY CHIRP

K. Yasutome*, T. Hara, H. Maesaka[2], K. Soutome[2], H. Tanaka, E. Iwai[2], I. Inoue[3]
RIKEN SPring-8 Center, Hyogo, Japan
[2]also at Japan Synchrotron Radiation Research Institute, Sayō, Japan
[3]also at University of Tokyo, Chiba, Japan

Abstract

We experimentally demonstrate the generation of sub-femtosecond hard XFEL pulses by recompressing the electron bunch in front of the undulators, which encourages time-resolved spectroscopy toward the attosecond regime. Space-charge fields and wakefields of accelerating structures induce a reverse-energy chirp, in which high-energy electrons locate in the bunch head, and it becomes pronounced for high-peak current bunches. At SACLA, we use a Double Bend Achromat lattice of the BL2 dogleg to compress the reverse-chirped bunches. R_{56} is tunable from negative to positive values by changing the bending angle, and thus the electron beam orbit and transverse envelope downstream are unchanged.Thanks to this simple tuning knob of the bunch recompression, normal SASE operation is quickly switched to sub-femtosecond operation mode in a highly reproducible manner. This scheme is also applicable to the other facilities having a similar setup. In this presentation, we overview the recompression scheme of the electron bunch with a reverse-energy chirp at SACLA, and highlight the experimental results, which show the XFEL pulse duration is below 1 fs, and pulse energy reaches around 60 μJ.

INTRODUCTION

Recent advances in time-resolved measurements of microscopic systems have reached the attosecond regime, corresponding to the timescale of electronic motion in atoms and molecules [1]. One promising application of attosecond pulses is structural and electronic-damage-free measurement [2], enabled by pulses short enough to outrun electronic damage.

We demonstrated the generation of sub-femtosecond XFEL pulses by further compressing the electron bunch upstream of the undulator section at the compact XFEL facility SACLA. Additional compression is achieved using a two-double-bend-achromat (two-DBA) dogleg, which provides a positive R_{56} to an electron bunch with a reverse energy chirp, where higher-energy electrons are located at the bunch head. The reverse energy chirp is produced primarily by geometrical wakefields and secondarily by longitudinal space-charge effects. To confirm sub-femtosecond pulse generation, we use a diagnostic based on nonlinear amplified spontaneous emission (ASE) [3], which indicates pulse durations in the sub-femtosecond regime with pulse energies up to 60 μJ.

* yasutome@spring8.or.jp

Various approaches to attosecond pulse generation have been proposed at XFEL facilities [4–11]. In particular, our method was inspired by the approach proposed by Yan *et al.* [10], in which the electron bunch is recompressed upstream of the undulator section using a compression arc. In their approach, longitudinal space-charge effects play a key role in producing the reverse energy chirp. A related concept was also proposed by Huang *et al.* [4], in which nonlinear compression of a low-charge bunch was used to produce ultrashort current spikes.

In contrast to these approaches, the present method is characterized by its operational simplicity and flexibility. An electron bunch with a reverse energy chirp can be further compressed using the positive R_{56} generated by the two-DBA dogleg. This R_{56} can be tuned simply by changing the bending angles while keeping the quadrupole strengths unchanged, thereby maintaining the transverse beam envelope and orbit at the downstream undulator section. Our method enables independent tuning of R_{56}, which controls the pulse duration, while preserving the transverse XFEL lasing conditions. As a result, the operation can be switched rapidly and reproducibly between the standard SASE and the sub-femtosecond modes.

SUB-FEMTOSECOND GENERATION SCHEME

Figure 1 shows a schematic illustration of the sub-femtosecond pulse-generation scheme and the corresponding beamline configuration at SACLA. The electron bunch, with a charge of 150 pC, is compressed to a peak current of approximately 10 kA using a three-stage chicane-based bunch-compression system. At the entrance of the final bunch compressor (BC3), the longitudinal phase space is nearly linear, as shown in Fig. 1(a). A high-current spike is then formed at the exit of BC3, as shown in Fig. 1(b). At this stage, the typical duration of the core of the electron bunch is on the order of 10–20 fs [12].

As the electron bunch is accelerated in the main C-band linac, the tail portion of the bunch experiences both geometrical wakefields and longitudinal space-charge (LSC) effects, whereas the head portion is affected predominantly by LSC. These collective effects induce an energy modulation along the bunch, resulting in a reverse energy chirp as illustrated in Fig. 1(c).

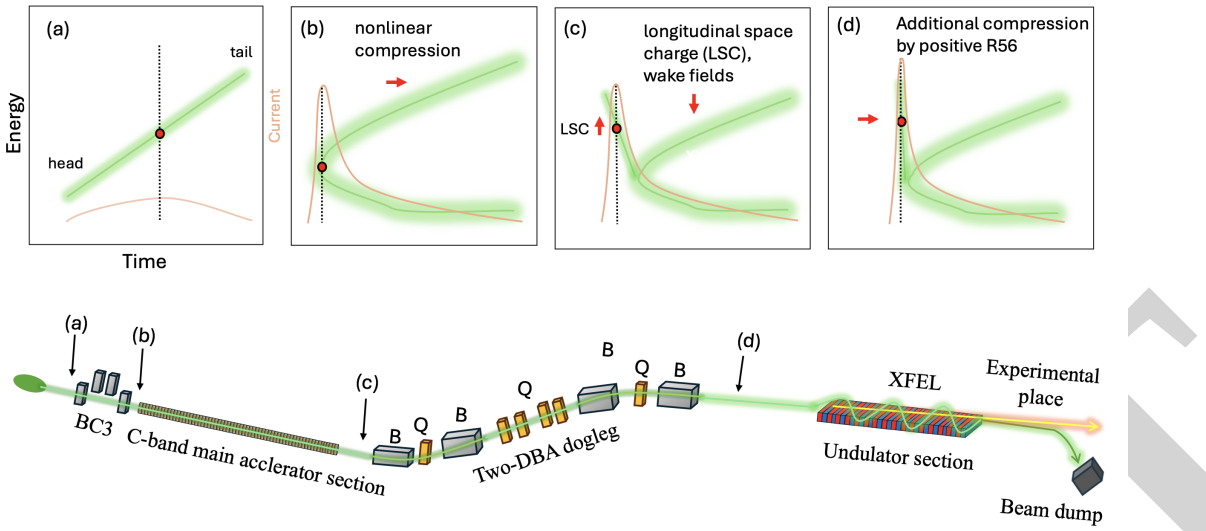

Figure 1: Schematic illustration of the sub-femtosecond pulse generation scheme and the key beamline components at SACLA. (a) Longitudinal phase space of the electron bunch at the exit of the final bunch compressor (BC3). (b) Formation of a high-current spike through nonlinear compression. (c) Formation of reverse energy chirp induced by geometrical wakefields and longitudinal space-charge effects. (d) Additional compression of the lasing region using a positive R_{56} in the DBA dogleg, resulting in an ultrashort current spike. The lower panel shows the corresponding accelerator layout, including BC3, C-band linac, the two-DBA dogleg section, and the undulator section.

The contributions of geometrical wakefields and LSC are evaluated using analytical models based on pillbox-cavity approximations [13]. The results indicate that the energy modulation induced by wakefields is larger than that induced by LSC. Although the cavity geometry and bunch distribution are simplified in this model, these assumptions are not expected to significantly affect the relative contributions of the wakefield and space-charge effects.

An electron bunch with a reverse energy chirp cannot be compressed using the negative R_{56} of a conventional chicane-based bunch compressor, but can be compressed using the positive R_{56} provided by the two-DBA dogleg. When the bending angle is set to 1.5 degrees, the electron beam passes through the centers of the quadrupoles. In the standard SASE operation, the bending angle is adjusted to 1.545 degrees to satisfy the condition $R_{56} = 0\,\mu\text{m}$, thereby suppressing changes in the bunch length and mitigating emittance degradation due to coherent synchrotron radiation (CSR) [14]. For additional bunch compression, the bending angle is further adjusted to produce a positive R_{56}. Although changing the bending angle introduces dispersion leakage from each of the two DBA cells, these contributions have opposite signs and cancel each other when the phase advance between the quadrupoles in the two DBA sections is set to 2π.

TUNING FOR SUB-FEMTOSECOND GENERATION

We conducted an experiment to demonstrate sub-femtosecond pulse generation. The accelerator was tuned as follows:

- The bending angles of the two-DBA dogleg were adjusted to vary R_{56}.
- The number of active undulator segments was reduced from 17 to 8 or 7.
- The RF phase of the C-band accelerating structures upstream of BC3 was tuned to relax the bunch compression.
- The beam orbit at the undulator entrance and the upstream quadrupole strengths were optimized to maximize the XFEL intensity.

During the tuning, we used three optimization metrics: the probability of obtaining single-spike-like spectra, the XFEL beam pointing stability, and the XFEL intensity. The spectra were measured using a shot-by-shot spectrometer installed at the XFEL experimental station, and the XFEL beam position was measured using a screen monitor. Figure 2 shows the evolution of the spectral spike statistics, a representative single-shot spectrum.

In this experiment, the photon energy was set to 10 keV, and the accelerator parameters were varied from the standard SASE condition, $R_{56} = 0\,\mu\text{m}$, to additional bunch-compression modes. In the SASE mode, multi-spike spectra dominated because the lasing region of the electron bunch was much longer than the cooperation length, as shown in Fig. 2(a) and (c). After tuning the bending angles for additional compression in the two-DBA dogleg and reducing the number of active undulator segments from 17 to 8, the probability of obtaining single-spike-like spectra increased

significantly. The bunch compression at BC3 was then relaxed to improve the beam pointing stability to the 10–20% level, which was sufficient for the nonlinear ASE measurements.

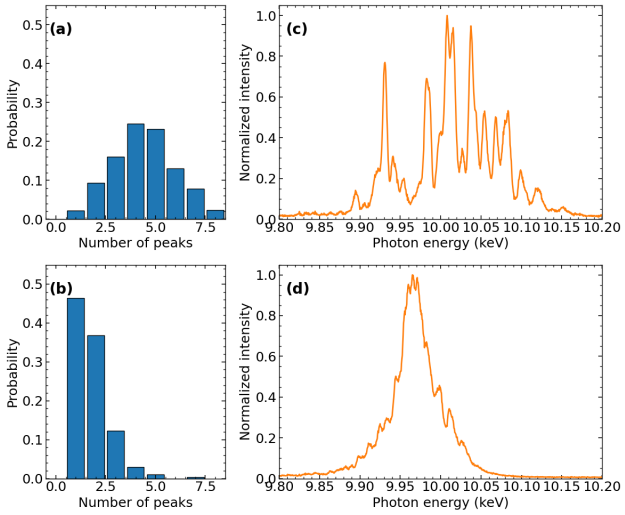

Figure 2: Characteristics of the XFEL spectrum under different accelerator operation conditions. (a, b) Probability distribution of the number of spectral peaks over 500 shots; (c, d) typical single-shot spectra; (a, c) Standard SASE operation with R_{56} =0 µm and 17 active undulators. (b, d) Additional bunch compression mode with R_{56} =760 µm, 8 active undulators, and relaxed bunch compression at BC3.

RESULTS

To confirm the generation of sub-femtosecond pulses, the XFEL pulse duration was evaluated using amplified spontaneous emission (ASE) from a 20 µm-thick copper foil irradiated by focused X-ray pulses [15]. Since the ASE yield strongly depends on the X-ray intensity, the pulse duration can be estimated from the measured pulse energy and focal beam size. The measurements were performed at SACLA BL2 [16]. The X-ray pulses were focused to nanometer-scale spots using Kirkpatrick–Baez optics [17], and the forward fluorescence signal was recorded with an MPCCD detector [18]. The shot-by-shot pulse energy was monitored upstream of the focusing optics [19], while the incident pulse energy was controlled using silicon attenuators. The focal beam size on the copper foil was evaluated by a knife-edge scan.

The machine conditions used for the ASE measurements are summarized as follows. Under the standard SASE condition (A), the longitudinal dispersion was set to R_{56} = 0 µm, with a beam size of 170 × 190 nm^2, 18 active undulators, and a pulse energy of 380 µJ. For the additional bunch-compression modes, the bunch compression at BC3 was relaxed. Under condition B (R_{56} = 760 µm), the beam size was 130 × 210 nm^2, with 8 active undulators and a pulse energy of 32 µJ. Under condition C (R_{56} = 980 µm), the beam size was reduced to 80 × 250 nm^2, with 7 active undulators and a pulse energy of 22 µJ. Under condition D (R_{56} = 1400 µm), the beam size was 80 × 290 nm^2, with 8 active undulators and a pulse energy of 40 µJ.

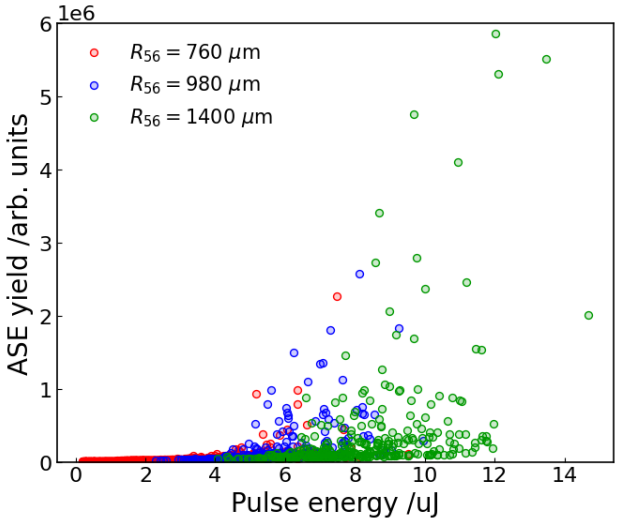

Figure 3: ASE yield as a function of the incident XFEL pulse energy for three additional bunch-compression conditions: R_{56} = 760 µm in red, 980 µm in blue, and 1400 µm in green.

Figure 3 shows the ASE yield as a function of the pulse energy for electron bunch recompression modes (condition B, C, and D). To confirm that the nonlinear signal did not originate from the beamline or the MPCCD detector, we compared the ASE signals measured with the copper foil placed at the focal position and at an off-focus position. The nonlinearity appeared only at the focal position, indicating that it originated from the ASE process.

Using the ASE threshold intensity [15], we estimated the XFEL pulse duration in this experiment. The threshold intensity was estimated to be 3 × 10^{19} W/cm^2, taking into account the difference in the photoabsorption cross section between 9.1 keV and 10.0 keV photons relative to the previous study [15].

The FWHM pulse durations in conditions of (B) and (C) are estimated to be below 1 fs, while that in condition (A) is 3 fs, and above 1 fs in condition (D) based on the ASE threshold obtained in this measurement. These results confirm the generation of sub-femtosecond pulses under conditions B and C. They indicate that condition D (R_{56} = 1400 µm) corresponds to an overcompressed condition, where the pulse duration becomes longer than that in condition B or C.

CONCLUSION

We have proposed and demonstrated a simple, robust scheme for generating sub-femtosecond XFEL pulses over several R_{56} settings. The pulse duration was evaluated using nonlinear ASE signals, confirming sub-femtosecond pulse generation at R_{56} = 760 µm and 980 µm. In this scheme, a reverse energy chirp is induced primarily by geometrical wakefields in the C-band accelerating structures, with an additional contribution from longitudinal space-charge effects. The electron bunch is subsequently compressed

using a positive R_{56} in a two-DBA dogleg. A key advantage of this method is that R_{56} can be tuned simply by adjusting the bending angles while keeping the quadrupole strengths unchanged, thereby preserving the transverse FEL lasing conditions. This enables rapid and reproducible switching between the conventional SASE mode and the sub-femtosecond operation mode. These features provide a practical route toward routine attosecond XFEL operation at existing and future facilities.

ACKNOWLEDGEMENTS

The authors are grateful to Jiawei Yan and Chenzhi Xu for fruitful discussions and their assistance with accelerator tuning for the sub-femtosecond pulse generation experiment at SACLA. The authors also thank Taito Osaka, Gota Yamaguchi, and Jumpei Yamada for their contributions to the ASE measurements performed in the experiment.

REFERENCES

[1] F. Krausz and M. Ivanov, "Attosecond phyiscs", *Rev. Mod. Phys.*, vol. 81, pp. 163, Feb. 2009. doi:10.1103/RevModPhys.81.163

[2] R. Neutze *et al.*, "Potential for biomolecular imaging with femtosecond X-ray pulses", *Nature*, vol. 406, pp. 752–757, Aug. 2000, doi:10.1038/35021099

[3] I. Inoue *et al.*, "Experimental demonstration of attosecond hard x-ray pulses", *arXiv*, Jun. 2025. doi:10.48550/arXiv.2506.07968

[4] S. Huang *et al.*, "Generating single-spike hard X-Ray pulses with nonlinear bunch compression in free-electron lasers", *Phys. Rev. Letts.*, vol. 119, pp. 154801, Oct. 2017, doi:10.1103/PhysRevLett.119.154801

[5] J. P. Duris *et al.*, "Tunable isolated attosecond X-ray pulses with gigawatt peak power from a free-electron laser", *Nat. Photonics*, vol. 14, pp. 30-36, Jan. 2020. doi:10.1038/s41566-019-0549-5

[6] Z. Zhang *et al.*, "Experimental demonstration of enhanced self-amplified spontaneous emission by photocathode temporal shaping and self-compression in a magnetic wiggler", *New J. Phys.*, vol. 22, pp. 083030, Aug. 2020. doi:10.1088/1367-2630/aba14c

[7] A. Marinelli *et al.*, "Experimental demonstration of a single-spike hard-X-ray free-electron laser starting from noise", *Appl. Phys. Lett.*, vol. 111, pp. 151101, Oct. 2020. doi:10.1063/1.4990716

[8] J. P. Duris *et al.*, "Controllable X-Ray pulse trains from enhanced self-amplified spontaneous emission", *Phys. Rev. Letts.*, vol. 126, pp. 104802, Mar. 2021. doi:10.1103/PhysRevLett.126.104802

[9] E. Prat *et al.*, "Coherent sub-femtosecond soft x-ray free-electron laser pulses with nonlinear compression", *APL Photonics*, vol. 8, Nov. 2023, doi:10.1063/5.0164666

[10] J. Yan *et al.*, "Terawatt-attosecond hard X-ray free-electron laser at high repetition rate", *Nat. Photonics*, vol. 18, Dec. 2024, doi:10.1038/s41566-024-01566-0

[11] E. Prat *et al.*, "Enhanced generation of single-spike hard x-ray free-electron laser pulses with lower charge and shorter electron beams in the injector", *Phys. Rev. Research*, vol. 7, pp. L042060, Dec. 2025. doi:10.1103/t8qq-h31p

[12] I. Inoue *et al.*, "X-ray Hanbury Brown-Twiss interferometry for determination of ultrashort electron-bunch duration", *Phys. Rev. Acc. Beams*, vol. 21, pp. 080704, Apr. 2018. doi:10.1103/PhysRevAccelBeams.21.080704

[13] K. Yokoya, "Short-range wake formulas for infinite periodic pill-box", KEK, Tsukuba, Japan, Rep. 90-21, May 1998.

[14] T. Hara *et al.*, "High peak current operation of x-ray free-electron laser multiple beam lines by suppressing coherent synchrotron radiation effects", *Phys. Rev. Acc. Beams*, vol. 21, pp. 040701, Apr. 2018. doi:10.1103/PhysRevAccelBeams.21.040701

[15] H. Yoneda *et al.*, "Atomic inner-shell laser at 1.5-angstrom wavelength pumped by an x-ray free-electron laser", *Nature*, vol. 524, pp. 446-449, 2015. doi:10.1038/nature14894

[16] M. Yabashi *et al.*, "Overview of the SACLA facility", *J. Synchrotron Radiat.*, vol. 22, pp. 477, May 2015. doi:10.1107/S1600577515004658

[17] I. Inoue *et al.*, "Nanofocused attosecond hard x-ray free-electron laser with intensity exceeding 10^{19}w/cm^2", *Optica*, vol. 12, no. 3, pp. 309-310, Mar. 2025. doi:10.1364/OPTICA.554954

[18] T. Kameshima *et al.*, "Development of an x-ray pixel detector with multi-port charge-coupled device for x-ray free-electron laser experiments", *Rev. Sci. Instrum.*, vol. 85, pp. 033110, Mar. 2014. doi:10.1063/1.4867668

[19] K. Tono *et al.*, "Overview of optics, photon diagnostics and experimental instruments at SACLA: development, operation and scientific applications", in *Proc. SPIE*, Advances in X-ray Free-Electron Lasers Instrumentation IV, vol. 10237, Prague, Czech Republic, May 2017. doi:10.1117/12.2268238